

Article

Rare-Earth Element Phase Associations in Four West Virginia Coal Samples

Rachel Yesenchak ¹, Shikha Sharma ^{1,*}, Christina Lopano ² and Scott Montross ³¹ Department of Geology & Geography, West Virginia University, Morgantown, WV 26506, USA² National Energy Technology Laboratory, U.S. Department of Energy, Pittsburgh, PA 15236, USA³ National Energy Technology Laboratory, U.S. Department of Energy, Albany, OR 97321, USA

* Correspondence: shikha.sharma@mail.wvu.edu; Tel.: +1-304-293-671

Abstract: Rare-earth elements are critical components of technologies used in renewable energy, communication, transportation, and national defense. Securing supply chains by developing domestic rare-earth resources, including coal and coal byproducts, has become a national priority. With some of the largest coal reserves in the country, states within the Appalachian Basin can play a key role in supplying these elements. Understanding rare-earth element phase associations and the processes that lead to enrichment in these coals will inform resource prospecting and recovery techniques. This study used sequential leaching in addition to scanning electron microscopy and energy-dispersive X-ray spectroscopy to identify rare-earth element modes of occurrence in WV coals. The results indicate that heavier elements have a stronger association with organic matter and that phosphate minerals are primary sources of both heavy and light rare-earth elements. However, these phases are shielded by a resistant aluminosilicate matrix that can impede the recovery of rare-earth elements using traditional methods.

Keywords: rare-earth elements (REE); coal; mode of occurrence



Citation: Yesenchak, R.; Sharma, S.; Lopano, C.; Montross, S. Rare-Earth Element Phase Associations in Four West Virginia Coal Samples. *Minerals* **2024**, *14*, 362. <https://doi.org/10.3390/min14040362>

Academic Editors: Jaroslav Dostal, Maria Economou-Eliopoulos, Martiya Sadeghi and David Lentz

Received: 19 February 2024

Revised: 22 March 2024

Accepted: 26 March 2024

Published: 29 March 2024



Copyright: © 2024 by the authors. Licensee MDPI, Basel, Switzerland. This article is an open access article distributed under the terms and conditions of the Creative Commons Attribution (CC BY) license (<https://creativecommons.org/licenses/by/4.0/>).

1. Introduction

Rare-earth elements and yttrium (REY) are essential components of many technologies fundamental to modern life and national security, such as cell phones, computers, and other electronics. These elements are also critical to U.S. and global decarbonization efforts due to their use in magnets for wind power generators and electric vehicle motors [1]. However, the U.S. is more than 90% import-reliant for REY [2], leaving supply chains vulnerable to disruption. To secure supply chains, new domestic REY resources must be developed. Coal and coal byproducts, including refuse and fly ash, can potentially serve as viable unconventional resources for REY. The enrichment of REY in select coal seams can rival that of conventional ores, and coal combustion in power plants further concentrates these elements in the resulting ash [3,4]. Major coal-producing states, such as West Virginia (WV), can utilize existing mining infrastructure and coal waste products to transition to the production of REY.

Rare-earth elements include the lanthanide series of elements (La through Lu), yttrium (Y), and sometimes scandium (Sc) due to similarities in physicochemical properties [5]. The elements are commonly partitioned into groups based on their ionic radius and atomic mass, either as light (La through Eu) or as heavy (Y and Gd through Lu) REY (LREE and HREY, respectively), or further refined to LREE (La through Sm), medium REY (MREY—Y and Eu through Dy), and HREE (Ho through Lu) [6,7]. Scandium does not fit neatly into the light, medium, and heavy classification scheme and will be discussed separately in this manuscript. The term “REE” will refer to lanthanide elements, and “REY” will refer to lanthanide elements plus Y.

In coal, REY can have organic and inorganic associations controlled by depositional conditions (e.g., sediment source geochemistry, synchronous volcanic inputs, redox conditions) and processes acting on the coal during or after diagenesis (e.g., metamorphism, meteoric or hydrothermal fluid infiltration) [7–9]. Inorganically associated REY can be present as crystalline minerals or non-crystalline mineraloids or adsorbed to the surfaces of clay minerals, while organically associated REY are bonded to or adsorbed onto organic compounds [10–13]. The first step in assessing coal deposits as REY resources is to understand REY concentrations and elemental modes of occurrence in order to relate their mineral phases to the aforementioned depositional, diagenetic, and epigenetic processes of enrichment. This information can then be used to identify economically promising coal seams based on their history of deposition and coalification. Identifying the REY modes of occurrence can also help predict the behavior of these elements during coal combustion and inform the design of efficient techniques to extract REY from coal and coal byproducts [11,14]. Sequential leaching is a standard method to identify the elemental modes of occurrence in rocks, including coal. The technique involves using a series of targeted solvents to dissolve individual mineral and organic phases, releasing the elements associated with each phase. Then, the leachate from each step in the sequence is analyzed separately to quantify the elements of interest released in that step. Solvents commonly include ammonium acetate or sodium acetate to target exchangeable cations, hydrofluoric acid to target silicates, nitric acid to target pyrite and phosphates, hydrogen peroxide to target organics, and hydrochloric acid to target carbonates, oxides, and monosulfides [15–19].

With a centuries-long history of coal extraction and utilization, states within the Appalachian Basin are well positioned to contribute to the nation's supply of REY. Studies suggest that coals and coal byproducts in the basin are especially promising as unconventional REY resources. A study by Lin et al. [20] using coal geochemistry data in the USGS CoalQual database found that central Appalachian Basin coals may serve as economically viable sources of REY. Generally, fly ash generated from Appalachian Basin coals has higher total REY (TREY) concentrations than Illinois and Powder River Basin ashes [21]. Critical REY, elements whose demand exceeds supply, accounted for 34%–38% of the TREY [21]. To develop Appalachian Basin coals as a resource for REY, it is imperative to understand elemental phase associations to better ascertain the provenance of REY in coal and how they translate to REY recovery techniques. This study used a sequential leaching methodology adapted from Tessier et al. [19] and Riley et al. [18], in addition to scanning electron microscopy and energy-dispersive X-ray spectroscopy (SEM-EDS), to identify the REY modes of occurrence in WV coals, providing insights into the elemental behaviors that can ultimately be leveraged to aid Appalachian Basin states in transitioning to the production of REY.

2. Materials and Methods

Four coal samples acquired from the West Virginia Geologic and Economic Survey (WVGES) were subjected to sequential leaching to identify the REY modes of occurrence. Samples were sourced from the Upper Kittanning, Sewell, and Fire Clay coal seams (2 different Fire Clay samples were used, coming from Fayette and Raleigh counties). A bulk sample from each seam was comminuted to a grain size of $\leq 150 \mu\text{m}$ and homogenized. Sample characteristics, including formation names, geologic ages, and ash yields (a proxy for inorganic content), are shown in Table 1. Although the bulk samples were initially identified as coal, the high ash yield of the Sewell sample suggests that it is not strictly coal. The sample was collected from a coal mine but may be a coal-adjacent carbonaceous claystone/shale or a mixture of interbedded coal and carbonaceous partings.

Table 1. Coal sample characteristics.

Coal Seam	Formation Name	Geologic Age	Ash Yield (%)
Upper Kittanning	Allegheny	Upper-middle Pennsylvanian	17.7
Fayette Fire Clay	Kanawha	Lower-middle Pennsylvanian	16.1
Raleigh Fire Clay	Kanawha	Lower-middle Pennsylvanian	6.6
Sewell	New River	Lower Pennsylvanian	56.1

The samples used in this study come from Pennsylvanian-aged coal seams in the northern and central Appalachian Basin. The proto-Appalachian Basin began developing about 1.1 billion years ago on continental crust extending along the margin of the proto-Atlantic Ocean. During the Allegheny orogeny (approximately 330–265 million years ago), a collision between southern Laurentia and Gondwana formed the Appalachian Mountains [22,23]. Subsidence west of the mountains created an elongated foreland basin, which was subsequently filled with clastic sediments that generally thickened toward the southeast. Sediments sourced from the Appalachian Mountains to the east and the Canadian craton to the north were deposited by fluvial channels and deltaic fans across a coastal plain that occasionally experienced shallow-marine flooding [22,23].

The coal seams represented in this study range from the lower- to upper-middle Pennsylvanian. Lower Pennsylvanian strata represent transgressive sequences with a depositional strike that sits parallel to the Appalachian Mountains. In West Virginia, lower Pennsylvanian formations are dominated by thick intervals of quartzose sandstone [22]. Middle Pennsylvanian strata were deposited in coastal and deltaic environments with episodes of marine inundation [22,24]. These rock sequences typically consist of coal, carbonaceous shale, mudstones, siltstones, minor sandstone, and sometimes carbonates [22]. Paleoclimate fluctuations during the middle Pennsylvanian resulted in more seasonal conditions compared to the persistently wet, tropical conditions of lower Pennsylvanian deposits [25–27]. Planar peat mires developing in mildly seasonal climates combined with marine incursions in the upper and upper-middle Pennsylvanian generally resulted in relatively high-ash, high-sulfur coals [24–27].

2.1. Bulk Sample Characterization

X-ray Diffraction: Qualitative X-ray diffraction (XRD) was carried out at the National Energy Technology Laboratory in Pittsburgh, PA, USA, to identify the primary crystalline mineral phases present in bulk coal (pre-reaction) samples and post-reaction residues. Samples were ground and sieved to a grain size of $\leq 45 \mu\text{m}$ and packed into stainless-steel back-loading cavity mounts. The samples were run on a Malvern PANalytical Aeris (Almelo, Netherlands) utilizing copper X-rays at 40 kV, 15 mA with a PixCel detector. The samples were scanned from 5 to 70 degrees (2θ) with a step size of 0.02 degrees and scan times of 118 s/step in continuous mode. Peak alignments, phase IDs, and mineral identifications were made using X'Pert HighScore Plus (version 5.1) software utilizing the ICDD PDF-4+ database.

Bulk Sample Digestion: Whole-coal REY and Sc concentrations were determined by digesting bulk samples using a proprietary sodium peroxide fusion method at the analytical lab at the WVU Energy Institute, Morgantown, PA, USA, followed by inductively coupled plasma mass spectrometry (ICP-MS) using U.S. EPA Method 200.8 [28]. Samples were analyzed using a PerkinElmer NexION 2000 ICP mass spectrometer (Shelton, CT, USA). Method detection limits (in $\mu\text{g/L}$) for the REY were Sc: 0.037; La: 0.003; Ce: 0.008; Pr: 0.003; Nd: 0.008; Sm: 0.004; Eu: 0.003; Gd: 0.003; Tb: 0.002; Dy: 0.004; Y: 0.004; Ho: 0.002; Er: 0.004; Tm: 0.002; Yb: 0.002; and Lu: 0.002.

Carbon and Sulfur: Total carbon and total sulfur analysis was performed by Pittsburgh Mineral & Environmental Technology in New Brighton, PA, USA. Bulk (pre-reaction) samples were comminuted to a grain size of $\leq 45 \mu\text{m}$. The powdered samples were scanned using the ELTRA CS800 Carbon-Sulfur Determinator (Newtown, PA, USA) after calibration using Alpha Resources standards. Two to three aliquots of each bulk sample and residue were scanned, and averaged results are provided.

Scanning electron microscopy–energy-dispersive X-ray spectroscopy: Scanning electron microscopy and energy-dispersive X-ray spectroscopy (SEM-EDS) were used to identify REY-bearing mineral phases in representative coal sample chips. The analysis was performed following the methods outlined in Montross et al. [29] and is briefly summarized below. Portable X-ray fluorescence (pXRF) was used as a screening tool to identify the most promising sample chips for SEM-EDS. Several chips from each coal sample were scanned using a handheld Olympus Vanta M-series portable X-ray Fluorescence Spectrometer (Tokyo, Japan) with 3-beam capability. Scans were run for 10 or 20 s per beam exposure (Beam 1, 10 kV; Beam 2, 20 kV; and Beam 3, 50 kV). General detection limits for REY on a whole-coal basis were La: 50 ppm; Ce: 65 ppm; Y: 1 ppm; and Nd: 80 ppm. Chips with higher La, Ce, and Y concentrations were prioritized for SEM-EDS. Selected coal chips were subjected to grinding and polishing using standard metallographic techniques to achieve a flat polished surface for imaging and X-ray analysis. A field-emission scanning electron microscope (JEOL IT700 HR) equipped with an energy-dispersive X-ray spectrometer (EDS, Oxford Instruments, Abingdon, United Kingdom) was used to observe the microstructure of coal samples and collect elemental data on the mineral phases present. The microscope was operated in low-vacuum mode with an accelerating voltage of 20–25 keV and a beam current of ~ 50 – 100 nA , and images were collected in backscattered mode (BSE). All samples were scanned in an x-y criss-cross pattern across the entire area ($\sim 8 \text{ cm}^2$) of the mounted sample. Standards-based quantitative EDS spot analysis and mapping were performed using certified rare-earth element standards for phosphates (REYP25-15+FC, Astimex Standards Ltd., Toronto, ON, Canada) and oxides (Standard block 194 #489, Geller Microanalytical Laboratory, Topsfield, MA, USA). Standard block #489 is certified to the ISO 9001 and ISO 17025 standards [30,31]. Scanning electron microscopy and EDS mapping were used to putatively identify REY-bearing minerals present in the coal samples. Point spectra, line spectra, and elemental maps were used to determine the composition of individual grains to facilitate the identification of mineral phases.

2.2. Sequential Extraction Procedure

A sequential leaching methodology was adapted from Tessier et al. [19] and Riley et al. [18] to target both the mineral and organic fractions of coal. The coal samples (including a replicate Fayette Fire Clay sample, referred to as “Fayette-R”) were crushed and sieved to obtain grain sizes $\leq 150 \mu\text{m}$. Eleven grams of each sample was placed inside a borosilicate beaker and washed using 225 mL of deionized water with continuous agitation for 18 h. Samples were washed in the same manner after each step of the sequential leaching process to remove any remaining reactants. After each step, the leachate was filtered using $0.45 \mu\text{m}$ Millipore filters, and 50 mL was transferred to polypropylene centrifuge tubes, where 0.5 mL of concentrated nitric acid was added to preserve the samples. The sequence of steps for sequential extraction was performed as follows: (1) The ion-exchangeable fraction was targeted using 88 mL of 1M sodium acetate solution, with continuous agitation at room temperature for 1 h. (2) Carbonates, oxides, monosulfides, and ferric iron species were targeted using 165 mL of 6M hydrochloric acid, with continuous agitation at room temperature for 18 h. (3) Pyrite and phosphates were targeted with 165 mL of 2M nitric acid, with continuous agitation for 18 h at room temperature. (4) The organic fraction was targeted by adding 33 mL of 0.02M nitric acid and 55 mL of 30% hydrogen peroxide adjusted to pH 2 with nitric acid. The solution was heated for 2 h with occasional agitation at $85 \text{ }^\circ\text{C}$. Then, another 33 mL portion of 30% hydrogen peroxide adjusted to pH 2 was added. Heating and occasional agitation continued for 3 additional hours. After the

mixture cooled, 55 mL of 3.2M ammonium acetate in 20% (*v/v*) nitric acid was added. The sample was then diluted to 225 mL and continuously agitated for 30 min. (5) Samples were transferred to conical polypropylene flasks, and silicates were targeted using 27.5 mL of concentrated hydrofluoric acid and 2.75 mL of concentrated hydrochloric acid, heated to 50 °C for 2 h, and then diluted to 165 mL with deionized water. Samples were left undisturbed for about 2 days, and then 30 mL of the leachate was transferred to a Teflon beaker, where it was neutralized with boric acid. The leachate was filtered using 60 mL Luer-Lok syringes with 0.45 µm PVDF filters attached. Leachate samples were analyzed by ICP-MS at the analytical lab at the West Virginia University (WVU) Energy Institute following U.S. EPA Method 200.8 [28] to quantify the REY released in each stage of the extraction process. A simplified flow diagram of the sequential leaching procedure is presented in Supplemental Figure S1.

3. Results

3.1. XRD

The primary mineral phases identified using qualitative XRD are shown in Table 2. All bulk patterns exhibited a high background, attributed to the amorphous carbon matrix of the coal, preventing the full quantification of all minerals present in the sample. Quartz and various mixtures of clay minerals (e.g., montmorillonite, illite, kaolinite, glauconite) were identified in all four whole-coal bulk samples. Pyrite was identified in the Upper Kittanning and Raleigh samples. Calcite was also present in the Upper Kittanning sample, as well as szomolnokite, a sulfate mineral that likely formed through pyrite oxidation [32]. In the post-reaction residual solids, hieratite (a potassium fluorosilicate) and potassium salts were identified in all four samples. A zirconium dioxide phase was tentatively identified in the Fayette residue. The XRD patterns of the pre-reaction samples and post-reaction residual solids are shown in Supplemental Figure S2A–D.

Table 2. Crystalline phases identified during qualitative XRD of bulk pre-reaction coal samples.

Coal Sample	Crystalline Phases Identified
Upper Kittanning	quartz, kaolinite, montmorillonite, glauconite, calcite, pyrite, szomolnokite
Fayette Fire Clay	quartz, kaolinite, illite, nontronite/montmorillonite
Raleigh Fire Clay	quartz, kaolinite/halloysite, illite/nacrite, montmorillonite, pyrite
Sewell	quartz, kaolinite, illite

3.2. Carbon and Sulfur

Total carbon and total sulfur were reported on a weight percent basis for bulk (pre-reaction) coal samples. The total carbon content was 36.17% for Sewell, 63.18% for Upper Kittanning, 73.42% for Fayette, and 78.61% for Raleigh. The total sulfur content was 0.36% for Sewell, 6.25% for Upper Kittanning, 0.41% for Fayette, and 0.44% for Raleigh.

3.3. SEM-EDS

Several chips from each coal sample were analyzed via pXRF before SEM-EDS analysis. The element concentrations determined by pXRF are shown in Table 3. Although pXRF measurements of trace elements may not be highly accurate, the relative concentrations can be used to select the most promising REY-bearing samples for SEM-EDS analysis [29].

Table 3. pXRF results reported in parts per million (ppm). The Chip column indicates the number of sample chips analyzed. A decimal indicates different sides of the same chip.

Coal Sample	Chip No.	Mg	Al	Si	P	S	K	Ca	Ti	V	Cr	Mn	Fe	Co	Ni	Cu	Zn	As
Upper Kittanning	1	ND	99,011	188,741	161	40,555	23,883	14,271	3954	122	51	80	17,601	ND	25	158	117	ND
	2	ND	28,291	34,554	61	85,706	3420	3016	2210	108	ND	58	81,475	534	13	18	38	194
	3	3580	86,320	130,554	119	33,471	13,208	1372	4618	360	92	64	27,118	248	93	114	350	48
Fayette Fireclay	1.1	ND	37,773	22,611	56	14,613	805	1957	584	47	ND	91	1943	ND	13	56	14	ND
	1.2	ND	27,190	26,464	55	14,798	1799	853	899	77	ND	61	2031	ND	13	53	10	ND
	2	3476	6544	6075	65	21,631	101	1241	930	93	ND	21	1270	12	ND	28	ND	ND
	3	ND	61,376	33,869	148	13,218	1342	1320	603	55	ND	52	2273	ND	8	49	10	ND
Raleigh Fireclay	4	4664	8317	6250	96	26,997	67	1574	874	73	ND	24	1574	15	ND	62	ND	ND
	1	4070	9025	29,140	138	15,461	255	497	2757	ND	ND	ND	4806	ND	5	41	18	3
	2	ND	4416	3387	55	17,292	ND	1413	183	ND	ND	26	3167	ND	12	27	7	ND
	3	2338	4279	4655	120	17,447	34	643	353	ND	ND	19	2752	ND	ND	30	8	ND
Sewell	1	ND	110,201	162,467	172	5887	17,835	724	1961	97	52	37	10,659	84	51	74	27	ND
	2	ND	86,403	108,513	104	5985	9785	782	2188	ND	ND	ND	4705	ND	23	59	14	ND
	3.1	2844	86,404	123,458	86	10,213	10,242	1423	4652	267	ND	36	5669	ND	31	77	17	ND
	3.2	ND	102,473	139,554	178	15,035	16,490	2690	5393	167	55	40	9470	58	31	91	21	ND
	4.1	ND	99,069	136,417	227	16,629	18,929	2079	4516	ND	93	ND	11,025	76	31	116	19	ND
	4.2	4274	84,182	115,920	113	13,993	7391	2004	8271	345	51	29	6209	45	36	71	20	ND
Coal Sample	Chip No.	Se	Rb	Sr	Y	Zr	Nb	Mo	Ba	La	Ce	Pr	Nd	W	Hg	Pb	Th	U
Upper Kittanning	1	ND	241	166	22	112	7	ND	396	93	145	157	ND	ND	ND	72	20	ND
	2	6	14	45	24	27	ND	17	122	ND	ND	ND	221	14	30	12	14	12
	3	3	140	75	19	138	ND	ND	478	127	186	ND	ND	ND	ND	60	18	6
Fayette Fireclay	1.1	2	10	41	15	8	ND	5	78	60	ND	ND	ND	ND	4	21	31	18
	1.2	1	18	42	15	13	ND	6	136	86	89	ND	ND	ND	ND	20	33	16
	2	ND	7	57	44	24	ND	ND	104	ND	ND	ND	131	63	43	5	24	10
	3	3	8	41	15	7	ND	ND	82	ND	ND	ND	ND	ND	ND	23	29	18
Raleigh Fireclay	4	ND	7	50	47	17	ND	ND	79	ND	ND	80	107	99	64	12	33	12
	1	1	2	79	36	59	ND	ND	89	ND	ND	ND	ND	ND	ND	8	31	14
	2	ND	ND	137	17	ND	ND	ND	90	48	ND	ND	ND	ND	ND	3	34	24
	3	ND	2	83	12	4	ND	4	74	ND	ND	ND	ND	ND	ND	6	34	18
Sewell	1	ND	110	123	46	78	ND	ND	278	91	93	ND	ND	ND	ND	21	ND	4
	2	ND	45	96	34	37	ND	ND	175	106	105	ND	ND	ND	ND	17	16	11
	3.1	ND	74	103	28	68	8	4	288	ND	129	183	212	ND	ND	20	21	11
	3.2	ND	158	218	39	97	ND	7	410	153	141	ND	ND	ND	ND	34	27	6
	4.1	ND	182	238	43	114	5	ND	503	132	143	ND	217	ND	ND	23	23	ND
	4.2	ND	92	116	28	85	7	ND	356	ND	ND	ND	ND	ND	ND	19	20	11

Rare-earth element bearing minerals identified using SEM-EDS are described in Table 4. Small grains of REY-phosphates, including monazite and xenotime, were found distributed in clay matrices. Rare-earth elements were also found co-located with sulfides and precipitates such as calcium oxalate and barite. Backscattered electron images showing examples of distinct REY-bearing minerals identified in the Sewell and Upper Kittanning samples are shown in Figure 1. Elemental maps and EDS peaks for these minerals are shown in Supplemental Figures S3A,B (Sewell) and S4A,B (Upper Kittanning). The elemental maps in Figure 2 show La concentrated in suspected barite, co-located with Ti, and lightly dispersed throughout an area containing clay and possible sulfides in the Fayette sample. Elemental maps showing LREE and P dispersed among clay layers in the Raleigh sample are shown in Figure 3.

Table 4. REY-bearing minerals identified using SEM-EDS.

Sample	REY-Bearing Minerals Identified
Upper Kittanning	La, Ce, Pr, Nd, Sm, Gd, Lu in monazite grains <5 μm
	LREE co-located with framboidal pyrite
Fayette	La lightly dispersed throughout an area containing Fe-rich clay and possible sulfides; concentrated in suspected barite and co-located with Ti
Raleigh	LREE and P dispersed in clay layers with abundant Fe-oxides
Sewell	Y, Gd, Sc in xenotime <5 μm
	Yb, Sc in Ca-oxalate in organic matter pore space
	La, Ce, Tb, Yb, Lu associated with an area of mixed sulfides (Fe, Pb, Cu, Ni, Se)
	Y in xenotime grains ≤5 μm
	Yb in an unidentified Ca-S mineral

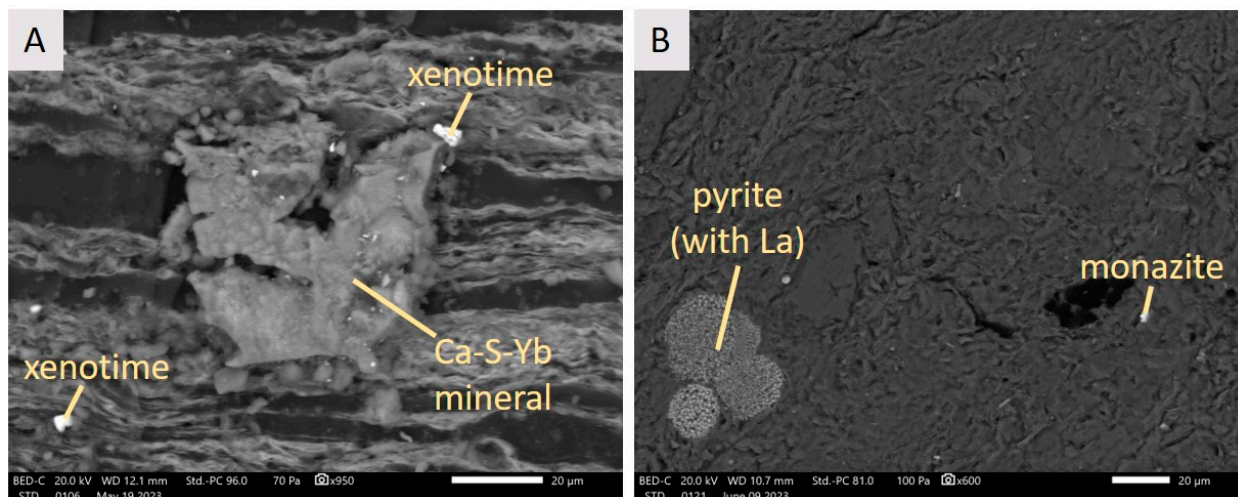


Figure 1. Backscattered electron images of a coal matrix and examples of discrete REY-bearing minerals. (A) Xenotime grains and an Yb-bearing Ca-S mineral in the Sewell sample. (B) A monazite grain and La co-located with pyrite framboids in the Upper Kittanning sample.

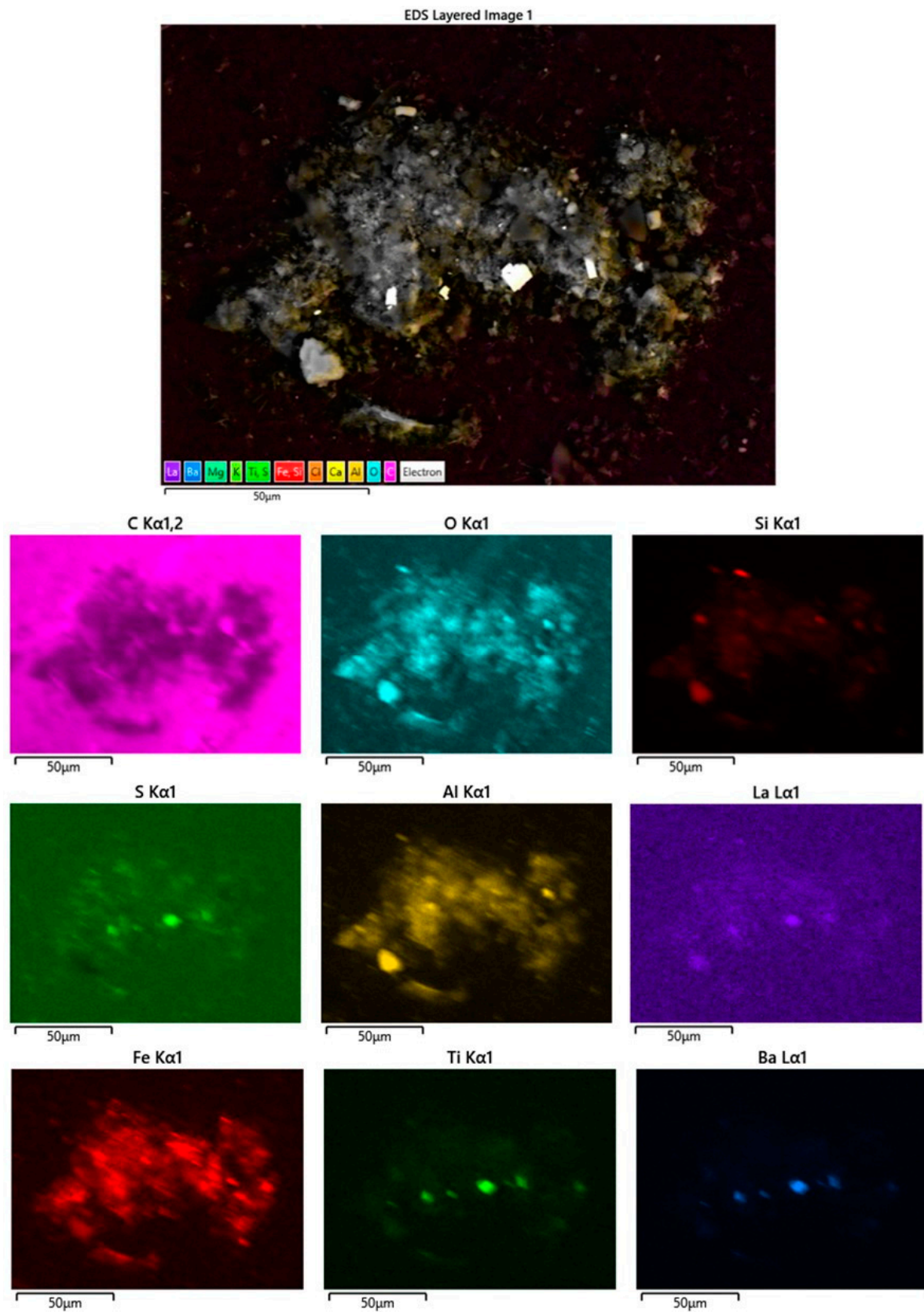


Figure 2. Elemental maps from the Fayette sample showing La lightly dispersed throughout an area of Fe-bearing clay, concentrated in suspected barite, and co-located with Ti.

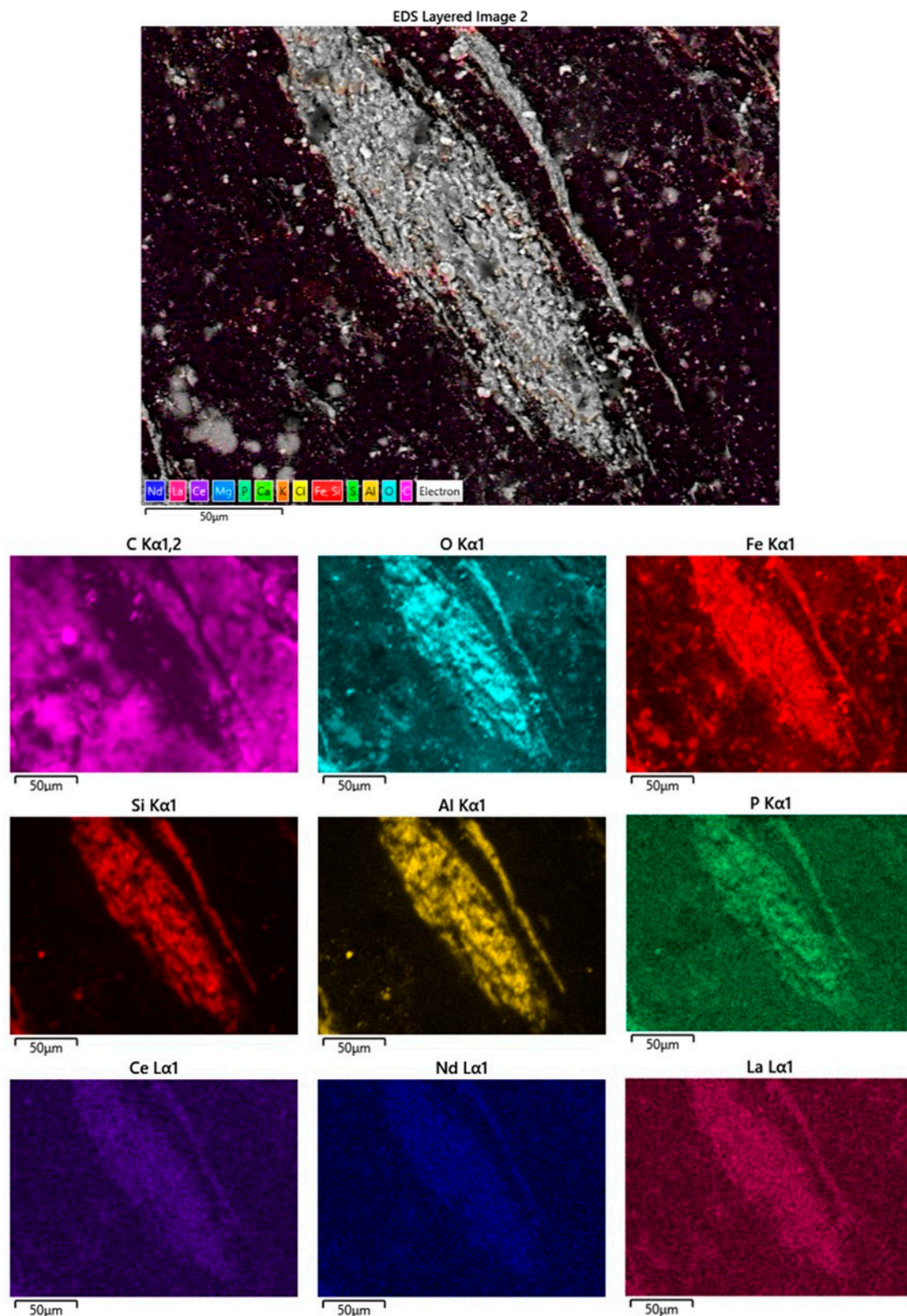


Figure 3. Elemental maps showing LREE and P dispersed among clay layers in the Raleigh sample.

3.4. Bulk Sample Rare-Earth Element Concentrations

Bulk samples were submitted for digestion and ICP-MS analysis to determine their whole-coal REY concentrations. The results are shown in Table 5. Sewell had the highest TREY concentration at 306.5 ppm, followed by Fayette with 64.3 ppm, Upper Kittanning

with 62.3 ppm, and Raleigh with 54.7 ppm. As shown in Figure 4, LREE account for the majority of TREY in the Sewell, Upper Kittanning, and Raleigh samples. Medium REY account for the largest proportion of TREY in the Fayette sample (about 44%). Less than 11% of TREY in each sample are composed of HREE.

Table 5. Bulk sample rare-earth element concentrations (reported in ppm).

Sample	Sc	La	Ce	Pr	Nd	Sm	Eu	Gd	Tb	Dy	Y	Ho	Er	Tm	Yb	Lu	TREY
Upper Kittanning	5.97	7.29	16.79	2.10	8.68	1.99	0.43	2.38	0.39	2.51	15.70	0.56	1.59	0.23	1.46	0.22	62.31
Sewell	19.48	55.59	110.27	13.67	53.28	10.37	2.04	9.74	1.38	7.72	31.88	1.48	4.11	0.60	3.85	0.54	306.53
Fayette	8.05	5.91	12.39	1.57	6.74	1.86	0.49	2.82	0.56	4.02	21.10	0.90	2.71	0.39	2.49	0.36	64.31
Raleigh	2.07	6.37	14.34	1.79	7.66	1.79	0.37	2.31	0.38	2.40	13.72	0.53	1.48	0.20	1.21	0.17	54.71

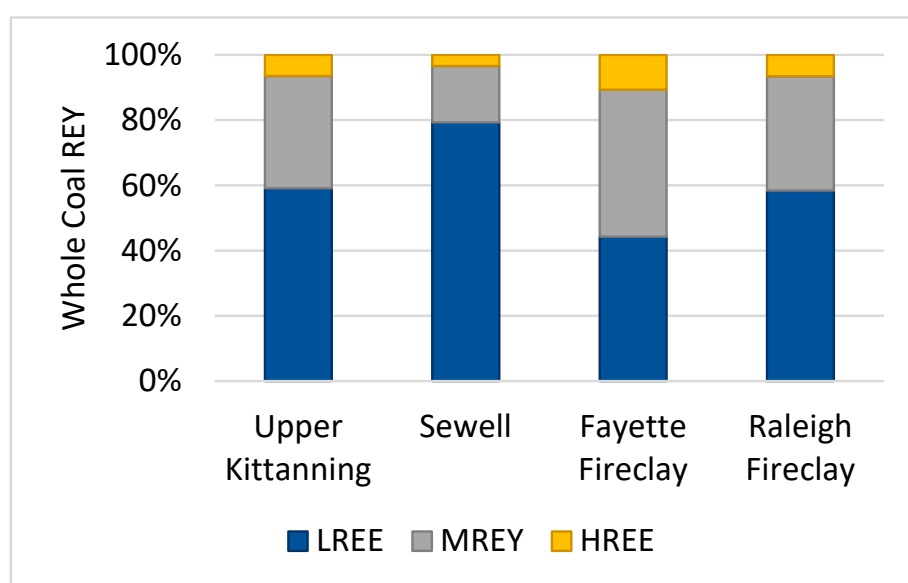


Figure 4. Distribution of light rare-earth elements (LREE), medium REY (MREY), and heavy REE (HREE) in bulk whole coal samples.

The rare-earth element concentration and distribution in coals are commonly evaluated against the average REY content of the upper continental crust (UCC). After normalizing elemental concentrations to the UCC, coals can be classified as having L-type (enriched in LREE), M-type (enriched in MREY), or H-type (enriched in HREE) distributions [7]. Figure 5 shows the REY distribution of each sample normalized to average UCC values as defined by Taylor and McLennan [33]. Sewell has an M-type distribution and is the only sample more enriched than the UCC for every element. The elements Nd through Dy are more than two times higher than UCC averages. The remaining coal samples have H-type REY distributions, which is common among world coals [7]. The Upper Kittanning and Raleigh samples are less enriched than the UCC for all elements. Fayette is more enriched than the UCC for the elements Dy through Lu (excluding Y, where coal/UCC = 0.96). All samples except for Upper Kittanning have negative Y anomalies, which is typical of U.S. coals [34].

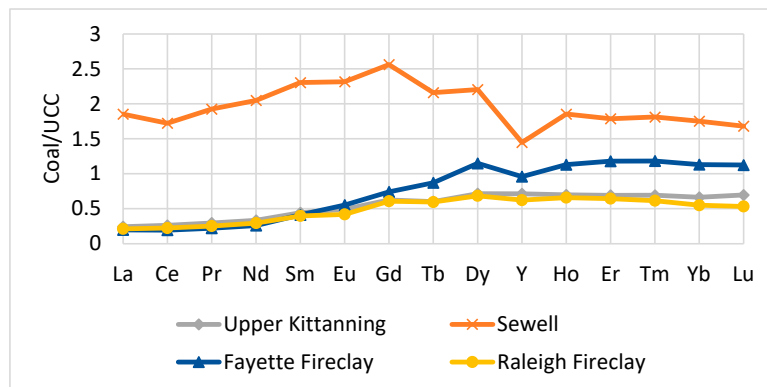


Figure 5. Whole-coal REY concentrations normalized to the upper continental crust (UCC).

3.5. Sequential Extraction

The concentration of TREY extracted from each coal sample during the full sequential leaching process is shown in Table 6. The overall extraction efficiency (percentage of TREY extracted) was 8.1% for Sewell, 22.1% for Upper Kittanning, 14.3% for Fayette, 14.1% for Fayette-R, and 13.8% for Raleigh. The low extraction efficiencies are largely due to the re-precipitation of silicate phases during the sequential leaching procedure (discussed later in this paper). The percentages of individual elements recovered from each sample during the full leaching process are shown in Figure 6. The recovery of Sc was similar for all samples, ranging from 13.1% to 17.4%. The recovery of La was even more similar for Upper Kittanning, Fayette, Fayette-R, and Raleigh, ranging from 14.5% to 16.0%. But the La recovery from Sewell was much lower at only 5.5%. In Sewell, MREY and HREE had significantly higher recoveries than LREE. However, in the remaining samples, HREE generally had lower recoveries than LREE and MREY.

Table 6. Rare-earth element concentrations extracted during the full sequential leaching process (reported in ppm).

Sample	Sc	La	Ce	Pr	Nd	Sm	Eu	Gd	Tb	Dy	Y	Ho	Er	Tm	Yb	Lu	TREY
Upper Kittanning	0.92	1.17	4.85	0.47	2.20	0.54	0.13	0.59	0.08	0.47	2.58	0.09	0.28	0.04	0.25	0.04	13.76
Sewell	3.40	3.03	7.08	0.84	3.72	1.12	0.29	1.46	0.20	1.20	4.15	0.23	0.67	0.09	0.59	0.08	24.75
Fayette	1.08	0.88	2.28	0.29	1.42	0.39	0.10	0.50	0.08	0.49	2.05	0.10	0.30	0.04	0.27	0.04	9.22
Fayette-R	1.05	0.85	2.27	0.29	1.40	0.39	0.09	0.50	0.07	0.48	2.00	0.10	0.29	0.04	0.26	0.03	9.07
Raleigh	0.31	0.99	2.47	0.29	1.26	0.27	0.06	0.29	0.04	0.23	1.34	0.05	0.13	0.02	0.11	0.02	7.56

Figure 7 shows the percentages of recoverable REY extracted from the coals during each step of the sequential leaching process. Less than 1% of recoverable TREY were extracted from the ion-exchangeable phase. Scandium and Y were present at concentrations above method detection limits in this phase in all samples. Among the lanthanide elements, Eu and Er were present in measurable concentrations in the ion-exchangeable leachate in four samples, Ho in three samples, Dy and Yb in two samples, and Gd, Tb, Tm, and Lu in one sample (only Sewell). The elements La through Sm were below detection limits in the leachate from this step for all samples. In the leachates for the remaining targeted coal fractions, all elements were present at concentrations above method detection limits. The majority of recoverable TREY were extracted from HCl-soluble phases in the Upper Kittanning, Fayette, and Fayette-R samples (51.3%, 59.2%, and 59.7% of TREY, respectively), while the majority of recoverable TREY in Sewell (60.2%) were extracted from the silicate fraction. In the Raleigh sample, the majority of recoverable TREY were split between the HCl-soluble and organic phases (47.8% and 32.6%, respectively). However, the recovery trends for individual elements vary. Recoverable Sc was largely divided among the HCl-

soluble, silicate, and organic fractions. A general trend of increasing recovery from the organic phase for heavier REY is observable in all samples.

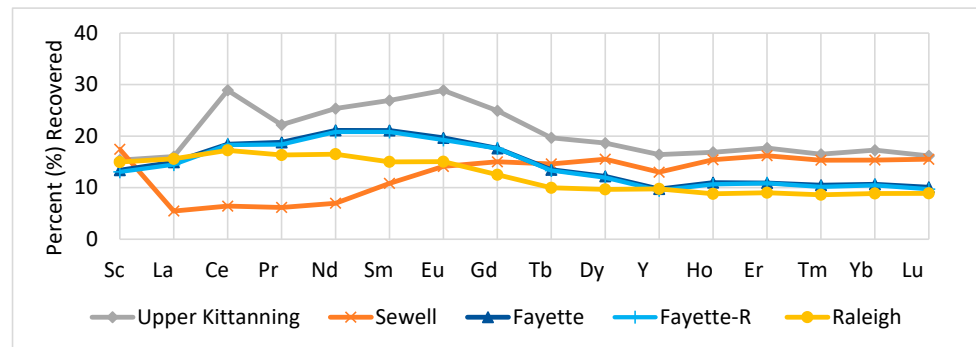


Figure 6. Percentage of each element recovered from the full sequential leaching process.

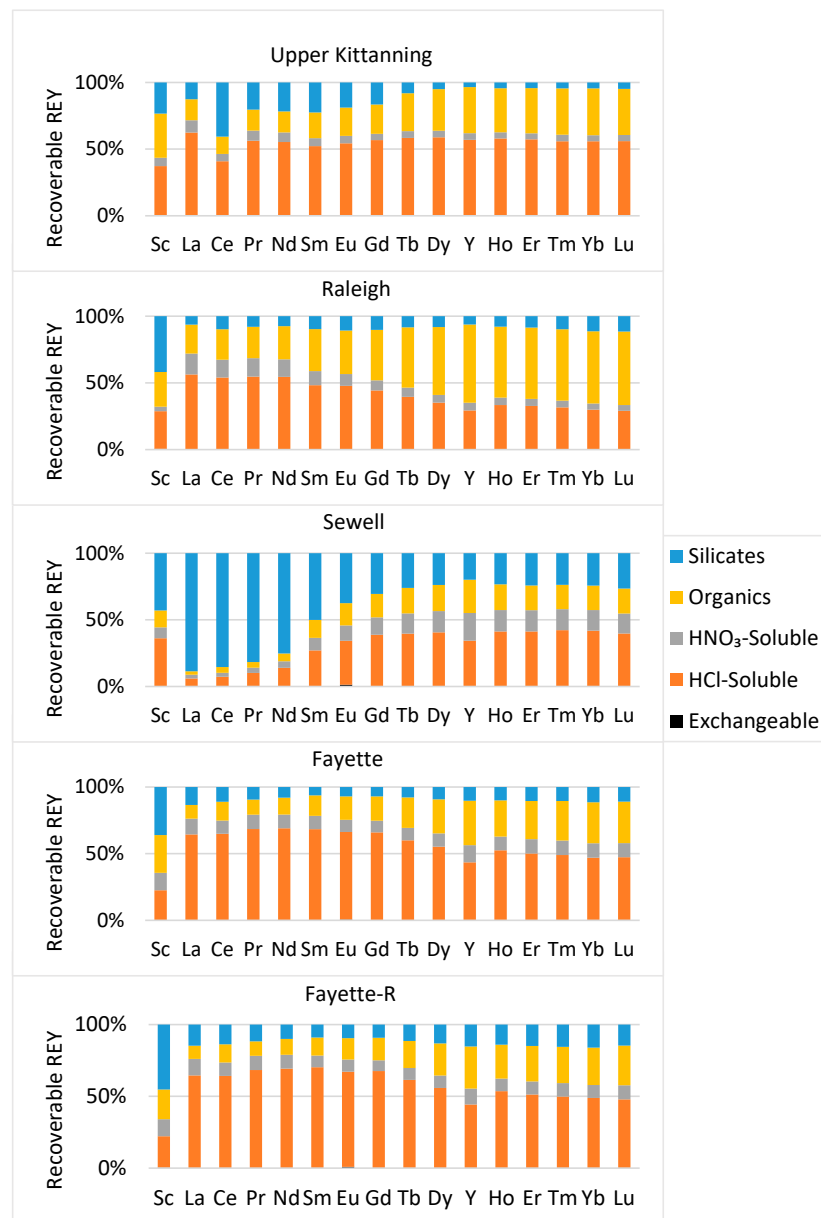


Figure 7. The percentage of REY extracted at each step of the leaching process (normalized to the total amount recovered).

4. Discussion

4.1. REY Enrichment and Distribution

Four main types of REY enrichment in coals, terrigenous, tuffaceous, infiltrational, and hydrothermal, are described by Seredin and Dai [7]. Terrigenous and tuffaceous enrichment occurs during the peat bog stage, with REY deposited into the mire by surface waters (terrigenous) or through falling volcanic ash and pyroclastics (tuffaceous). Enrichment by infiltration is a post-depositional process whereby REY are introduced into coal seams by circulating groundwater. Hydrothermal enrichment can occur during or after deposition as ascending hydrothermal fluids carry REY into coal seams or peat mires. A fifth enrichment type was suggested by Hower et al. [35], where REY in coal are derived from the original peat-forming plants. In some cases, a combination of enrichment types may be responsible for the REY content of a coal seam [36,37]. However, terrigenous enrichment is thought to be the primary source of REY in most coals and underclays [6,38]. The original REY mineral associations may remain in the coal or may be reworked in acidic peat mires or during coalification with the subsequent formation of new REY-bearing phases [37]. The total REY concentration generally correlates well with the ash yield, which can be used as a proxy for mineral matter in coal [38].

Light- and heavy-REY distribution in coal can be controlled by sediment source geochemistry, peat mire characteristics, and diagenetic or post-diagenetic processes. The ratio of LREE to HREE present in coal can sometimes be used to make inferences about the enrichment types or processes that have influenced a coal seam. Heavy REY form more stable complexes with organic matter than LREE and are therefore more likely to be associated with the organic fraction of coal [7,12,38–40]. Organically bound HREE can be displaced during diagenesis as chelating functional groups are lost, resulting in changes in the original LREE/HREE ratios if the HREE are subsequently leached from the coal [41,42]. However, the displaced HREE may also be reincorporated into authigenic mineral phases or bound to clays [6,42]. Light-to-heavy REY ratios can also be affected by the leaching of surrounding rocks or partings within the coal and hydrothermal fluids mobilizing and redistributing REY [43,44].

The LREE/HREE ratios (excluding Sc and Y) of the samples in this analysis range from 2.03 (Fayette) to 8.34 (Sewell). The LREE/HREE ratio of Sewell is notable. High LREE/HREE ratios are common in coals and related rocks of terrigenous origin, which often have L-type UCC-normalized REY distributions [7,37]. However, low-ash coals formed in ombrogenous mires may also have higher LREE/HREE ratios due to a lack of HREE-enriched detrital input [42]. The high ash yield of the Sewell sample indicates a significant detrital influence during deposition, which would account for the high LREE/HREE ratio. However, the sample also has an M-type UCC-normalized REY distribution (Figure 5). M-type distributions are common in coals influenced by acidic waters circulating within coal basins [7,37]. A weakly negative Ce anomaly and Gd maximum further support a fluid-based REY distribution in this sample [34]. The strongly negative Y anomaly may also result from fluid circulation. The literature suggests that, compared to Ho, Y is more likely to be leached and transported in solution due to weaker adsorption capabilities [45,46]. Mineral precipitates containing Yb were found in the Sewell sample using SEM-EDS. An Yb-bearing Ca-S mineral (shown in Figure 1A) appears to have been emplaced after deposition of the primary horizontal layers. Ytterbium in this mineral may have been sourced from the partial dissolution of the adjacent xenotime grain caused by acidic fluid flow.

The relatively low LREE/HREE ratio of the Fayette sample is also notable. Hower et al. [35] proposed that low LREE/HREE ratios may be a “ghost signature” of organically associated HREE in the coal-forming peat or early diagenetic precursors of bituminous coal. Shand et al. [47] investigated the cause of HREE enrichment in mildly acidic groundwaters in the Russian Far East and suggested that the weathering of zircon leached HREE and U into the fluids. A high U concentration in coal is generally associated with the presence of U-bearing detrital minerals such as zircon or with authigenic minerals and organically bound U sourced from groundwater [11,48,49]. The Fayette and Sewell samples contain

relatively high concentrations of U. When plotted against the ash yield (Figure 8), the U concentrations of Sewell, Upper Kittanning, and Raleigh appear to be influenced by non-volatile mineral matter content. However, the Fayette sample does not follow this trend, possibly indicating enhanced enrichment from fluids. Although U was not a focus of this study, it was included in the sequential extraction leachate analyses. While the extraction efficiency from the Fayette sample was low (15.3%), the majority of recoverable U was extracted from the HCl-soluble and organic phases (43.8% and 22.4%, respectively). With respect to common HCl-soluble mineral phases, U has been reported in association with REY-rich carbonates but is more often found in oxides, such as uraninite [11,48]. Uranium in an aqueous solution can be reduced to uraninite by Fe-rich smectite clays [50]. Iron-bearing smectite clay was tentatively identified in the Fayette sample by XRD analysis. Additional support for a fluid-based influence in the Fayette sample includes the relatively high W concentrations measured during pXRF, which range from undetectable to 99 ppm (Table 3). The published literature suggests that high W concentrations in coal are more likely to be supplied by aqueous solutions rather than by terrigenous sources [51–53]. Further, SEM-EDS revealed gold and platinum-group element mineralization in organic matter pore spaces and coal fractures, which could have been introduced by groundwater or hydrothermal fluids [54,55]. Finally, authigenic barite (identified via SEM-EDS) was found in association with suspected sulfides. Barite can be generated during the oxidative dissolution of sulfides in the presence of warm meteoric fluids [56].

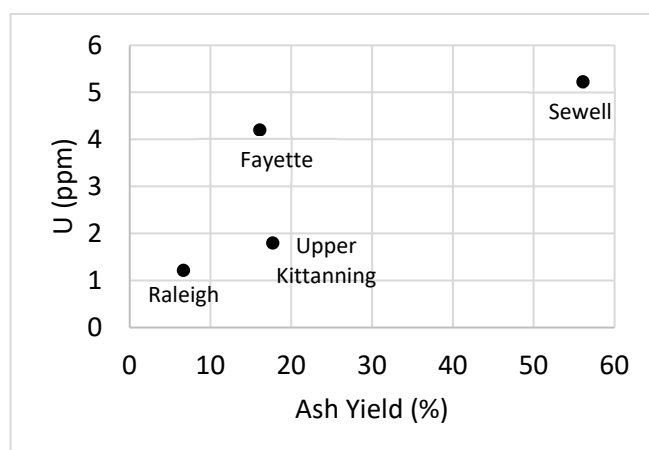


Figure 8. Plot of uranium versus ash yield (%) representing non-volatile mineral matter.

The Fayette sample was sourced from the Fire Clay coal seam, which has a complex history, including the deposition of a volcanic ash tonstein, groundwater leaching, and hydrothermal mineralization [36,55,57]. Coals underlying the tonstein can be enriched in TREY, at times exceeding 4000 ppm (ash basis), due to the groundwater leaching of the volcanic ash layer [57]. These coals are also commonly enriched in Zr [57]. The ash-basis TREY concentration of the Fayette sample is only 399 ppm, suggesting little to no influence from the tonstein. Zirconium was not analyzed during whole-rock digestion, but pXRF analysis found relatively low Zr concentrations (ranging from 7 to 24 ppm) in bulk sample chips, and a zirconium dioxide phase was tentatively identified using XRD in the post-reaction residual solids. Like Fayette, the Raleigh sample was also sourced from the Fire Clay coal seam. The Raleigh ash-basis TREY concentration is 822 ppm, more than twice as high as Fayette. Discrete REY minerals were not observed in this sample, but elemental mapping revealed LREE and P dispersed among Fe-bearing clay layers. Zirconium in the Raleigh sample ranged from undetectable to 59 ppm during pXRF scanning, but only three chips were analyzed. An abundance of iron oxides (identified using SEM-EDS) throughout the analyzed samples suggests oxidizing fluid flow.

The Upper Kittanning coal seam was deposited during a time of changing paleoclimate. The upper and upper-middle Pennsylvanian coals were generally formed in

topogenous peat mires during drier and more seasonal conditions than coals from the lower and lower-middle Pennsylvanian [25,26]. Marine and non-marine limestones, micrites, calcareous shales, and mudstones are typical of this time period in northern WV [25]. Non-marine, lacustrine limestones are sporadically associated with the Upper Kittanning coal seam [25,58]. The relatively neutral pH of peat mires at this time often resulted in high-S coals, although S contents in the Upper Pennsylvanian are variable [25]. The Upper Kittanning sample used in this study has a very high total S content (6.25 wt %), and several morphologies of pyrite were identified using SEM-EDS. Calcite was identified during XRD analysis. Groundwater interaction in a planer peat mire may have played a role in the REY distribution of the Upper Kittanning sample, but REY would not be highly mobile in relatively neutral waters. However, authigenic minerals such as carbonates could sequester REY displaced during diagenesis, including those formerly bound to organics as chelating functional groups are lost.

4.2. REY Phase Associations

Sequential leaching is a standard indirect method used to examine elemental modes of occurrence. Several studies have used the technique to identify REY phase associations in coal and coal-related strata. Li et al. [59] targeted REY in the carbonate, organic, silicate, sulfide, exchangeable, and water-soluble phases in Chinese coals of varying geologic ages. They concluded that the majority of REY were associated with silicate minerals [59]. A study on Appalachian Basin coal underclays and coarse refuse examined REY in water-soluble, exchangeable, acid-soluble, reducible, and oxidizable fractions [60]; however, less than a quarter of TREY were recovered from the samples. The authors concluded that the unrecovered REY are in apatitic phases and REY-phosphates. Using XRD and electron microscopy, they confirmed the presence of REY-bearing phosphates, including apatite, monazite, xenotime, crandallite, rhabdophane, and churchite [60]. Finkelman et al. [17] used sequential leaching to estimate the percentage of REY associated with different mineral phases in bituminous and low-rank world coals. They concluded that about 70% of LREE are found in phosphate minerals in bituminous coals, 20% are associated with clays, and 10% are associated with carbonates and organic matter. For HREY, they estimated that 50% are associated with phosphates, 20% with clays, and 30% with organic matter and carbonates. However, the percentage of REY recovered from each phase varied for individual samples [17].

In the present study, the overall extraction efficiencies were poor, with 74.9% to 93.4% of LREE and 82.4% to 90.1% of HREY remaining in the residuals (Figure 9). The low recovery was primarily due to the re-precipitation of silicate phases during the final stage of the sequential leaching procedure. During XRD analysis, hieratite, a K-bearing hexafluorosilicate, was identified in the post-reaction residuals of all four samples. Potassium salts were also identified in all sample residuals. The presence of these phases in the residual solids indicates the re-precipitation of clays and possibly other silicate phases.

Although REY extraction from the silicate phases cannot be considered complete, it is assumed that the REY extracted from the other major mineral phases targeted (ion-exchangeable, HCl-soluble, and sulfides) represent the majority of REY associated with those phases. Based on this assumption, the current results are similar to the estimates provided by Finkelman et al. [17] if clay-shielded REY-bearing phases are considered. Studies on coal and related strata, including underclays, overburden, and refuse, have shown that REY-bearing phosphate minerals (e.g., monazite, xenotime, and rhabdophane) are commonly found within clay matrix pore spaces [61–63]. Most of these REY-phosphates were observed to be less than 5 μm in length [61–63]. This is consistent with SEM-EDS results for the present study, where REY-phosphate grains $\leq 5 \mu\text{m}$ in length were identified dispersed throughout the clay matrices. For the sequential extraction experiment, samples were ground and passed through a 150 μm , 100-mesh sieve, meaning that many REY-phosphate minerals would still be shielded by aluminosilicate phases. Additionally, some of the REY initially in solution during the hydrofluoric acid step of the sequential leaching

procedure would likely have been sequestered during the re-precipitation of silicates and related phases.

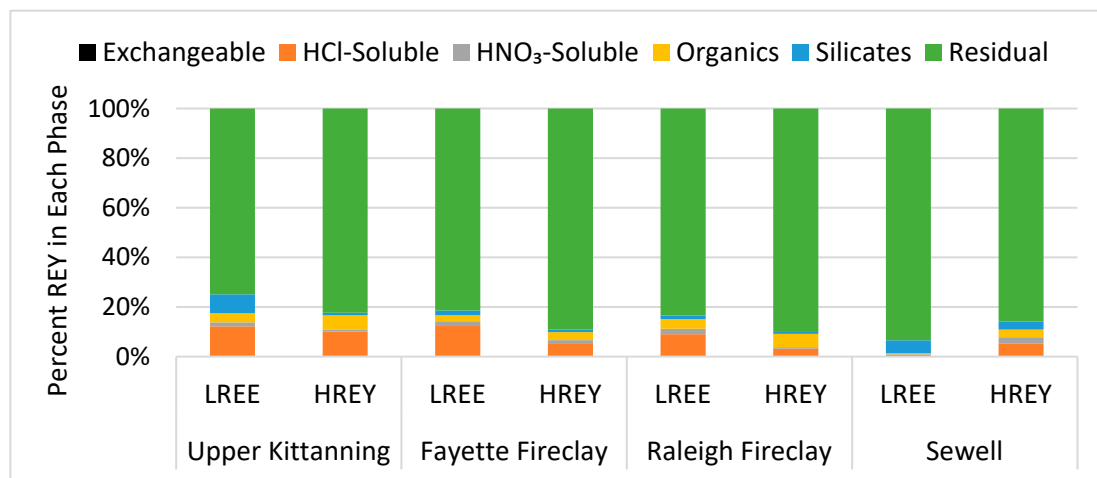


Figure 9. Percentages of LREE and HREY recovered from each leaching phase and percent remaining in the residual.

In all samples except for Sewell, the percentage of LREE recovery exceeded that of HREY recovery. The same trend was found by Finkelman et al. [17], who attributed the difference to a more significant proportion of HREY associated with organic matter, a phase that was not explicitly targeted during their sequential leaching experiment. In the present study, REY in the organic fraction were directly targeted. The relatively high ash yield and low total carbon content of the Sewell sample indicate that Sewell contained less organic matter than the other samples. It appears that the dissolution of organic matter was more complete in Sewell, which could explain why HREY recovery exceeded LREE recovery only in this sample. Regardless, a general trend of increasing organic association for heavier REY is apparent in all samples, as shown in Figure 7.

Little to no REY were recovered from the ion-exchangeable phase (Figure 7). Among the four samples, the recovery of ion-exchangeable REY was greatest for Sewell, with MREY having a better recovery than LREE or HREE. This may be due to the relatively high clay mineral content of the sample providing more ion-exchange sites. Alternatively, the exchangeable elements could have been sorbed onto organic matter, as the literature suggests that MREY have a greater tendency to sorb onto organics than other REY [7].

For all samples except Sewell, the HCl-soluble fraction provided the best overall REY recovery, particularly for LREE. In Sewell, a greater proportion of MREY and HREY were recovered from this fraction. In the Upper Kittanning sample, recovery from the HCl-soluble fraction was similar for all lanthanide elements (Figure 7), ranging from 41% (Ce) to 62% (La) of recoverable REY. It is the only sample where carbonate minerals (calcite) were identified (using XRD). While carbonates were the major phase targeted during the HCl leaching step, oxides, monosulfides, and ferric iron species may also have been dissolved. Additionally, smectite-group clays can have varying solubility in HCl. Komadel et al. [64] found that the dissolution rate of montmorillonite in a boiling HCl solution increased with increasing substitution of Fe and Mg for octahedral Al. Similarly, Hu et al. [65] demonstrated the increased HCl solubility of smectites with increasing cation substitution of Al. The study showed that HCl concentrations of 7N or higher can dissolve the more heavily substituted clays even at room temperature (21 °C). An HCl concentration of 5N had little to no effect on the samples at 21 °C [65]. The implications for the present study are unclear, as a concentration of 6M HCl was used to leach samples at room temperature. It is possible that smectite-group clays were partially dissolved during the HCl leaching step. Montmorillonite was identified in the Upper Kittanning, Raleigh, and Fayette samples during XRD analysis.

The recovery of REY from the HNO₃-soluble fraction was relatively low, ranging from 6.0% to 11.3% of recoverable TREY and 3.3% to 13.0% of Sc. Typically, HNO₃ is used to target sulfide minerals (e.g., pyrite) in coal during sequential leaching experiments [15,16,18,66], but Finkelman et al. [17] state that the majority of HNO₃-soluble REY are likely present in phosphates. A study by Grawunder et al. [67] found that pyrite samples were depleted in LREE as compared to MREY and HREE. However, in the present study, LREE had better recovery during the HNO₃ extraction step in all three samples where pyrite was identified during SEM-EDS analysis (Upper Kittanning, Fayette, and Raleigh). Since SEM-EDS revealed light, medium, and heavy REY in association with sulfide minerals (e.g., pyrite and chalcopyrite), it is possible that all of the HNO₃-soluble REY were recovered from sulfides. But the contribution of REY (particularly LREE) from the dissolution of phosphates cannot be ruled out. In the Fayette sample, the recovery from HNO₃-soluble phases was similar for all REY, ranging from 8.7% (Gd) to 12.8% (Y) of recoverable elements. In Sewell, MREY and HREE did have higher recovery from HNO₃-soluble phases than LREE. But the overall recovery of LREE in the Sewell sample was low, likely due to the relative abundance of LREE (79% of TREY) in the bulk sample combined with a high aluminosilicate content that shielded the primary LREE-bearing minerals. In fact, the vast majority of recoverable LREE in the Sewell sample were extracted during the final stage of the leaching process targeting silicate phases (80.9%). Although recovery was much lower, the Upper Kittanning sample produced a vaguely similar trend, where the silicate fraction accounted for a larger proportion of recoverable LREE than for MREY or HREE. In both the Fayette and Raleigh samples, recovery from the silicate fraction was low and relatively consistent for all REY. However, the recovery of REY from silicate phases cannot be considered complete. Further, some of the REY recovered during this step would not have been directly bound to silicates but rather present in minerals originally shielded by the aluminosilicate matrix.

4.3. Improving REY Extraction Efficiency

The sequential leaching methodology used in this paper was adapted from previous studies that were designed for Australian coals [18] and non-coal rocks [19]. This method was not adequate to recover the entirety of REY from the samples used in this study. The recovery of REY from Appalachian Basin coals, coal byproducts, and coal-adjacent rocks will require an efficient method to dissolve or otherwise decompose silicate and organic phases. Comminuting samples to a smaller grain size could yield better results by exposing minute REY-bearing minerals previously shielded by the aluminosilicate matrix. However, this may not be feasible since many REY-bearing phases identified in Appalachian Basin coal and underclay samples are present in mineral grains less than 5 µm in length [61–63]. A more viable option is to pre-treat coals using calcination to dehydroxylate clays and burn off volatile compounds, including organic matter. However, this method of pre-treatment appears to have a greater impact on the recovery of LREE than HREY [68,69]. Alternatively, the alkaline digestion of silicates before acid leaching of REY can be used to improve the recovery of both LREE and HREY. Recent studies have found that utilizing alkaline solutions or roasting additives, such as NaOH or Na₂CO₃, can increase the REY yield during subsequent acid leaching [70–73].

5. Conclusions

Identifying the REY modes of occurrence in coal is a necessary first step in utilizing coal and coal byproducts as domestic REY resources. This study used sequential leaching and SEM-EDS to identify REY phase associations in four WV coal samples. The recovery of REY from the sequential leaching process was low due to the re-precipitation of silicate phases and the incomplete dissolution of organic matter, suggesting that traditional sequential leaching methodologies are not well suited to Appalachian coals. Although organic matter dissolution was not complete, a general trend of increasing organic association for heavier REY was observable in all samples. Small (≤ 5 µm) grains of REY-phosphates, including

monazite and xenotime, were found embedded in the aluminosilicate matrix, which at least partially shielded these minerals during the sequential leaching process.

The samples used in this study represent a diverse array of mineral assemblages, organic matter content, depositional conditions, and post-depositional processes present within the Appalachian Basin; however, only a small number of samples were analyzed in this study. Out of the four preliminary samples used in this study, Sewell had the highest TREY concentration on a whole-rock basis (306.5 ppm). The relatively large fraction of inorganic mineral matter (as indicated by an ash yield of 56%) in this sample can account for the overall elevated TREY content. The MREY-enrichment pattern suggests the influence of acidic fluid circulation, which may have further enhanced the overall TREY concentration. To fully understand the REY resource potential of the Sewell coal seam and other WV coals and coal-related rocks, additional research is necessary to assess variations in both lateral and vertical REY concentrations and phase associations.

Supplementary Materials: The following supporting information can be downloaded at <https://www.mdpi.com/article/10.3390/min14040362/s1>: Figure S1: Simplified flow diagram of the sequential leaching procedure.; Figure S2: X-ray diffraction patterns of the pre- and post-reaction samples; Figure S3: EDS maps and peaks for some REY-bearing minerals in the Sewell sample; Figure S4: EDS maps and peaks for some REY-bearing minerals in the Upper Kittanning sample.

Author Contributions: Conceptualization, S.S.; Methodology, S.S., S.M., C.L. and R.Y.; Validation, S.S., R.Y., S.M. and C.L.; Formal Analysis, R.Y.; Investigation, R.Y.; Resources, S.S., S.M., C.L. and R.Y.; Data Curation, R.Y.; Writing—Original Draft Preparation, R.Y.; Writing—Review and Editing, R.Y., S.S., C.L. and S.M.; Visualization, R.Y.; Supervision, S.S.; Project Administration, S.S. and R.Y.; Funding Acquisition, R.Y. and S.S. All authors have read and agreed to the published version of the manuscript.

Funding: This research was funded by the IsoBioGem Laboratory, the Thomas E. Garner Student Award in Geology grant from West Virginia University Department of Geology & Geography, and funds awarded through the American Association of Petroleum Geologists Grants-in-Aid Program (Donald F. Towse Memorial Grant and the Pittsburgh Association of Petroleum Geologists Named Grant).

Data Availability Statement: Data are contained within the article and Supplementary Materials.

Acknowledgments: We would like to thank Jim Britton and the West Virginia Geological and Economic Survey for providing the coal samples used in this research, Vikas Agrawal and Bennington Opdahl for their guidance and help in the lab and developing the experimental protocol, and Sophia O’Barr for performing pXRF analysis.

Conflicts of Interest: The authors declare no conflicts of interest.

References

1. U.S. Department of Energy. *Multi-Year Program Plan for Division of Minerals Sustainability*; U.S. Department of Energy Office of Fossil Energy and Carbon Management: Washington, DC, USA, 2021.
2. U.S. Geological Survey. *Mineral Commodity Summaries 2022*; U.S. Geological Survey: Reston, VA, USA, 2022; p. 202.
3. Balam, V. Rare Earth Elements: A Review of Applications, Occurrence, Exploration, Analysis, Recycling, and Environmental Impact. *Geosci. Front.* **2019**, *10*, 1285–1303. [[CrossRef](#)]
4. Franus, W.; Wiatros-Motyka, M.M.; Wdowin, M. Coal Fly Ash as a Resource for Rare Earth Elements. *Environ. Sci. Pollut. Res.* **2015**, *22*, 9464–9474. [[CrossRef](#)] [[PubMed](#)]
5. Wu, S.; Wang, L.; Zhao, L.; Zhang, P.; El-Shall, H.; Moudgil, B.; Huang, X.; Zhang, L. Recovery of Rare Earth Elements from Phosphate Rock by Hydrometallurgical Processes—A Critical Review. *Chem. Eng. J.* **2018**, *335*, 774–800. [[CrossRef](#)]
6. Seredin, V.V. Rare Earth Element-Bearing Coals from the Russian Far East Deposits. *Int. J. Coal Geol.* **1996**, *30*, 101–129. [[CrossRef](#)]
7. Seredin, V.V.; Dai, S. Coal Deposits as Potential Alternative Sources for Lanthanides and Yttrium. *Int. J. Coal Geol.* **2012**, *94*, 67–93. [[CrossRef](#)]
8. Crowley, S.S.; Stanton, R.W.; Ryer, T.A. The Effects of Volcanic Ash on the Maceral and Chemical Composition of the C Coal Bed, Emery Coalfield, Utah. *Org. Geochem.* **1989**, *14*, 315–331. [[CrossRef](#)]
9. Mastalerz, M.; Drobnia, A.; Eble, C.; Ames, P.; McLaughlin, P. Rare Earth Elements and Yttrium in Pennsylvanian Coals and Shales in the Eastern Part of the Illinois Basin. *Int. J. Coal Geol.* **2020**, *231*, 103620. [[CrossRef](#)]

10. Dai, S.; Hower, J.C.; Finkelman, R.B.; Graham, I.T.; French, D.; Ward, C.R.; Eskenazy, G.; Wei, Q.; Zhao, L. Organic Associations of Non-Mineral Elements in Coal: A Review. *Int. J. Coal Geol.* **2020**, *218*, 103347. [[CrossRef](#)]
11. Dai, S.; Finkelman, R.B.; French, D.; Hower, J.C.; Graham, I.T.; Zhao, F. Modes of Occurrence of Elements in Coal: A Critical Evaluation. *Earth-Sci. Rev.* **2021**, *222*, 103815.
12. Laudal, D.A.; Benson, S.A.; Addleman, R.S.; Palo, D. Leaching Behavior of Rare Earth Elements in Fort Union Lignite Coals of North America. *Int. J. Coal Geol.* **2018**, *191*, 112–124. [[CrossRef](#)]
13. Lin, R.; Bank, T.L.; Roth, E.A.; Granite, E.J.; Soong, Y. Organic and Inorganic Associations of Rare Earth Elements in Central Appalachian Coal. *Int. J. Coal Geol.* **2017**, *179*, 295–301. [[CrossRef](#)]
14. Querol, X.; Klika, Z.; Weiss, Z.; Finkelman, R.; Alastuey, A.; Juan, R.; López-Soler, A.; Plana, F.; Kolker, A.; Chenery, S.R. Determination of Element Affinities by Density Fractionation of Bulk Coal Samples. *Fuel* **2001**, *80*, 83–96. [[CrossRef](#)]
15. Dai, S.; Chou, C.-L.; Yue, M.; Luo, K.; Ren, D. Mineralogy and Geochemistry of a Late Permian Coal in the Dafang Coalfield, Guizhou, China: Influence from Siliceous and Iron-Rich Calcic Hydrothermal Fluids. *Int. J. Coal Geol.* **2005**, *61*, 241–258. [[CrossRef](#)]
16. Finkelman, R.B.; Palmer, C.A.; Krasnow, M.R.; Aruscavage, P.J.; Sellers, G.A.; Dulong, F.T. Combustion and Leaching Behavior of Elements in the Argonne Premium Coal Samples. *Energy Fuels* **1990**, *4*, 755–766. [[CrossRef](#)]
17. Finkelman, R.B.; Palmer, C.A.; Wang, P. Quantification of the Modes of Occurrence of 42 Elements in Coal. *Int. J. Coal Geol.* **2018**, *185*, 138–160. [[CrossRef](#)]
18. Riley, K.W.; French, D.H.; Farrell, O.P.; Wood, R.A.; Huggins, F.E. Modes of Occurrence of Trace and Minor Elements in Some Australian Coals. *Int. J. Coal Geol.* **2012**, *94*, 214–224. [[CrossRef](#)]
19. Tessier, A.; Campbell, P.G.C.; Bisson, M. Sequential Extraction Procedure for the Speciation of Particulate Trace Metals. *Anal. Chem.* **1979**, *51*, 844–851. [[CrossRef](#)]
20. Lin, R.; Soong, Y.; Granite, E.J. Evaluation of Trace Elements in U.S. Coals Using the USGS COALQUAL Database Version 3.0. Part I: Rare Earth Elements and Yttrium (REY). *Int. J. Coal Geol.* **2018**, *192*, 1–13. [[CrossRef](#)]
21. Taggart, R.K.; Hower, J.C.; Dwyer, G.S.; Hsu-Kim, H. Trends in the Rare Earth Element Content of U.S.-Based Coal Combustion Fly Ashes. *Environ. Sci. Technol.* **2016**, *50*, 5919–5926. [[CrossRef](#)]
22. Ruppert, L.F.; Ryder, R.T. (Eds.) *Coal and Petroleum Resources in the Appalachian Basin: Distribution, Geologic Framework, and Geochemical Character*; U.S. Geological Survey: Reston, VA, USA, 2014.
23. Greb, S.F.; Pashin, J.C.; Martino, R.L.; Eble, C.F. Appalachian Sedimentary Cycles during the Pennsylvanian: Changing Influences of Sea Level, Climate, and Tectonics. In *Resolving the Late Paleozoic Ice Age in Time and Space*; Fielding, C.R., Frank, T.D., Isbell, J.L., Eds.; Geological Society of America: Boulder, CO, USA, 2008; Volume 441, pp. 235–248. ISBN 978-0-8137-2441-6.
24. Martino, R.L. Stratigraphy and Depositional Environments of the Kanawha Formation (Middle Pennsylvanian), Southern West Virginia, U.S.A. *Int. J. Coal Geol.* **1996**, *31*, 217–248. [[CrossRef](#)]
25. Cecil, C.B. *Paleoclimate Controls on Carboniferous Sedimentation and Cyclic Stratigraphy in the Appalachian Basin*; US Geological Survey Open File Report; US Geological Survey: Reston, VA, USA, 1998.
26. Cecil, C.B.; Stanton, R.W.; Neuzil, S.G.; Dulong, F.T.; Ruppert, L.F.; Pierce, B.S. Paleoclimate Controls on Late Paleozoic Sedimentation and Peat Formation in the Central Appalachian Basin (U.S.A.). *Int. J. Coal Geol.* **1985**, *5*, 195–230. [[CrossRef](#)]
27. DiMichele, W.A.; Cecil, C.B.; Montañez, I.P.; Falcon-Lang, H.J. Cyclic Changes in Pennsylvanian Paleoclimate and Effects on Floristic Dynamics in Tropical Pangaea. *Int. J. Coal Geol.* **2010**, *83*, 329–344. [[CrossRef](#)]
28. Creed, J.T.; Brockhoff, C.A.; Martin, T.D. *U.S. EPA Method 200.8: Determination of Trace Elements in Waters and Wastes by Inductively Coupled Plasma-Mass Spectrometry*; Revision 5.4; Environmental Monitoring Systems Laboratory Office of Research and Development: Cincinnati, OH, USA, 1994.
29. Montross, S.N.; Bagdonas, D.; Paronish, T.; Bean, A.; Gordon, A.; Creason, C.G.; Thomas, B.; Phillips, E.; Britton, J.; Quillian, S.; et al. On a Unified Core Characterization Methodology to Support the Systematic Assessment of Rare Earth Elements and Critical Minerals Bearing Unconventional Carbon Ores and Sedimentary Strata. *Minerals* **2022**, *12*, 1159. [[CrossRef](#)]
30. International Organization for Standardization. Quality Management Systems Requirements (ISO Standard No. 9001:2015). 2015. Available online: <https://www.iso.org/standard/62085.html> (accessed on 19 February 2024).
31. International Organization for Standardization. General Requirements for the Competence of Testing and Calibration Laboratories (ISO/IEC Standard No. 17025:2017). 2017. Available online: <https://www.iso.org/standard/66912.html> (accessed on 19 February 2024).
32. Rao, C.P.; Gluskoter, H.J. *Occurrence and Distribution of Minerals in Illinois Coals*; Circular 476; Illinois State Geological Survey: Urbana, IL, USA, 1973.
33. Taylor, S.R.; McLennan, S.M. *The Continental Crust: Its Composition and Evolution*; Blackwell Scientific Publishers: Boston, MA, USA, 1985.
34. Dai, S.; Graham, I.T.; Ward, C.R. A Review of Anomalous Rare Earth Elements and Yttrium in Coal. *Int. J. Coal Geol.* **2016**, *159*, 82–95. [[CrossRef](#)]
35. Hower, J.C.; Eble, C.F.; Backus, J.S.; Xie, P.; Liu, J.; Fu, B.; Hood, M.M. Aspects of Rare Earth Element Enrichment in Central Appalachian Coals. *Appl. Geochem.* **2020**, *120*, 104676. [[CrossRef](#)]
36. Hower, J.C.; Eble, C.F.; Dai, S.; Belkin, H.E. Distribution of Rare Earth Elements in Eastern Kentucky Coals: Indicators of Multiple Modes of Enrichment? *Int. J. Coal Geol.* **2016**, *160–161*, 73–81. [[CrossRef](#)]

37. Arbuzov, S.I.; Chekryzhov, I.Y.; Finkelman, R.B.; Sun, Y.Z.; Zhao, C.L.; Il'enok, S.S.; Blokhin, M.G.; Zarubina, N.V. Comments on the Geochemistry of Rare-Earth Elements (La, Ce, Sm, Eu, Tb, Yb, Lu) with Examples from Coals of North Asia (Siberia, Russian Far East, North China, Mongolia, and Kazakhstan). *Int. J. Coal Geol.* **2019**, *206*, 106–120. [[CrossRef](#)]
38. Eskenazy, G.M. Rare Earth Elements in a Sampled Coal from the Pirin Deposit, Bulgaria. *Int. J. Coal Geol.* **1987**, *7*, 301–314. [[CrossRef](#)]
39. Aide, M.T.; Aide, C. Rare Earth Elements: Their Importance in Understanding Soil Genesis. *ISRN Soil Sci.* **2012**, *2012*, 783876. [[CrossRef](#)]
40. Eskenazy, G. Sorption of Trace Elements on Xylain: An Experimental Study. *Int. J. Coal Geol.* **2015**, *150–151*, 166–169. [[CrossRef](#)]
41. Hatcher, P.G.; Clifford, D.J. The Organic Geochemistry of Coal: From Plant Materials to Coal. *Org. Geochem.* **1997**, *27*, 251–274. [[CrossRef](#)]
42. Hower, J.C.; Eble, C.F.; Hopps, S.D.; Morgan, T.D. Aspects of Rare Earth Element Geochemistry of the Pond Creek Coalbed, Pike County, Kentucky. *Int. J. Coal Geol.* **2022**, *261*, 104082. [[CrossRef](#)]
43. Dai, S.; Ren, D.; Chou, C.-L.; Li, S.; Jiang, Y. Mineralogy and Geochemistry of the No. 6 Coal (Pennsylvanian) in the Junger Coalfield, Ordos Basin, China. *Int. J. Coal Geol.* **2006**, *66*, 253–270. [[CrossRef](#)]
44. Dai, S.; Zhang, W.; Ward, C.R.; Seredin, V.V.; Hower, J.C.; Li, X.; Song, W.; Wang, X.; Kang, H.; Zheng, L.; et al. Mineralogical and Geochemical Anomalies of Late Permian Coals from the Fusui Coalfield, Guangxi Province, Southern China: Influences of Terrigenous Materials and Hydrothermal Fluids. *Int. J. Coal Geol.* **2013**, *105*, 60–84. [[CrossRef](#)]
45. Möller, P.; Morteani, G.; Dulski, P. Anomalous Gadolinium, Cerium, and Yttrium Contents in the Adige and Isarco River Waters and in the Water of Their Tributaries (Provinces Trento and Bolzano/Bozen, NE Italy). *Acta Hydrochim. Hydrobiol.* **2003**, *31*, 225–239. [[CrossRef](#)]
46. Bau, M.; Koschinsky, A.; Dulski, P.; Hein, J.R. Comparison of the Partitioning Behaviours of Yttrium, Rare Earth Elements, and Titanium between Hydrogenetic Marine Ferromanganese Crusts and Seawater. *Geochim. Cosmochim. Acta* **1996**, *60*, 1709–1725. [[CrossRef](#)]
47. Shand, P.; Johannesson, K.H.; Chudaev, O.; Chudaeva, V.; Edmunds, W.M. Rare Earth Element Contents of High pCO₂ Groundwaters of Primorye, Russia: Mineral Stability and Complexation Controls. In *Rare Earth Elements in Groundwater Flow Systems*; Johannesson, K.H., Ed.; Water Science and Technology Library; Springer: Dordrecht, The Netherlands, 2005; pp. 161–186. ISBN 978-1-4020-3234-9.
48. Seredin, V.V.; Finkelman, R.B. Metalliferous Coals: A Review of the Main Genetic and Geochemical Types. *Int. J. Coal Geol.* **2008**, *76*, 253–289. [[CrossRef](#)]
49. Wang, X.; Feng, Q.; Meng, Q.; Liu, F.; Cao, Q.; Liu, G. Distribution and Modes of Occurrence of Uranium in Coals of Eastern Yunnan, China. *Int. J. Coal Sci. Technol.* **2021**, *8*, 1262–1271. [[CrossRef](#)]
50. Tsarev, S.; Waite, T.D.; Collins, R.N. Uranium Reduction by Fe(II) in the Presence of Montmorillonite and Nontronite. *Environ. Sci. Technol.* **2016**, *50*, 8223–8230. [[CrossRef](#)] [[PubMed](#)]
51. Eskenazy, G.M. The Geochemistry of Tungsten in Bulgarian Coals. *Int. J. Coal Geol.* **1982**, *2*, 99–111. [[CrossRef](#)]
52. Etschmann, B.; Liu, W.; Li, K.; Dai, S.; Reith, F.; Falconer, D.; Kerr, G.; Paterson, D.; Howard, D.; Kappen, P.; et al. Enrichment of Germanium and Associated Arsenic and Tungsten in Coal and Roll-Front Uranium Deposits. *Chem. Geol.* **2017**, *463*, 29–49. [[CrossRef](#)]
53. Xiao, Z.; Cao, Y.; Jiang, W.; Zhou, P.; Huang, Y.; Liu, J. Minerals and Enrichment of W, Rb, and Cs in Late Permian Coal from Meitian Mine, Meitian Coalfield, Southern China by Magmatic Hydrothermal Fluids. *Minerals* **2018**, *8*, 504. [[CrossRef](#)]
54. Bullock, L.A.; Parnell, J.; Armstrong, J.G.T.; Perez, M.; Spinks, S. Gold in Irish Coal: Palaeo-Concentration from Metalliferous Groundwaters. *Minerals* **2020**, *10*, 635. [[CrossRef](#)]
55. Hower, J.C.; Berti, D.; Hochella, M.F.; Mardon, S.M. Rare Earth Minerals in a “No Tonstein” Section of the Dean (Fire Clay) Coal, Knox County, Kentucky. *Int. J. Coal Geol.* **2018**, *193*, 73–86. [[CrossRef](#)]
56. Fernández-Caliani, J.C.; Crespo, E.; Rodas, M.; Barrenechea, J.F.; Luque, F.J. Formation of Nontronite from Oxidative Dissolution of Pyrite Disseminated in Precambrian Felsic Metavolcanics of the Southern Iberian Massif (Spain). *Clays Clay Miner.* **2004**, *52*, 106–114. [[CrossRef](#)]
57. Hower, J.C.; Ruppert, L.F.; Eble, C.F. Lanthanide, Yttrium, and Zirconium Anomalies in the Fire Clay Coal Bed, Eastern Kentucky. *Int. J. Coal Geol.* **1999**, *39*, 141–153. [[CrossRef](#)]
58. Arkle, T., Jr. Stratigraphy of the Pennsylvanian and Permian Systems of the Central Appalachians. In *Carboniferous of the Southeastern United States*; Briggs, G., Ed.; Geological Society of America: Boulder, CO, USA, 1974; Volume 148, pp. 5–29, ISBN 978-0-8137-2148-4.
59. Li, D.; Tang, Y.; Deng, T.; Chen, K.; Liu, D. Geochemistry of Rare Earth Elements in Coal—A Case Study from Chongqing, Southwestern China. *Energy Explor. Exploit.* **2008**, *26*, 355–362. [[CrossRef](#)]
60. Bauer, S.; Yang, J.; Stuckman, M.; Verba, C. Rare Earth Element (REE) and Critical Mineral Fractions of Central Appalachian Coal-Related Strata Determined by 7-Step Sequential Extraction. *Minerals* **2022**, *12*, 1350. [[CrossRef](#)]
61. Montross, S.N.; Verba, C.A.; Chan, H.L.; Lopano, C. Advanced Characterization of Rare Earth Element Minerals in Coal Utilization Byproducts Using Multimodal Image Analysis. *Int. J. Coal Geol.* **2018**, *195*, 362–372. [[CrossRef](#)]
62. Montross, S.N.; Yang, J.; Britton, J.; McKoy, M.; Verba, C. Leaching of Rare Earth Elements from Central Appalachian Coal Seam Underclays. *Minerals* **2020**, *10*, 577. [[CrossRef](#)]

63. Zhang, W.; Honaker, R. Characterization and Recovery of Rare Earth Elements and Other Critical Metals (Co, Cr, Li, Mn, Sr, and V) from the Calcination Products of a Coal Refuse Sample. *Fuel* **2020**, *267*, 117236. [[CrossRef](#)]
64. Komadel, P.; Schmidt, D.; Madejová, J.; Čížek, B. Alteration of Smectites by Treatments with Hydrochloric Acid and Sodium Carbonate Solutions. *Appl. Clay Sci.* **1990**, *5*, 113–122. [[CrossRef](#)]
65. Hu, B.; Zhang, C.; Zhang, X. The Effects of Hydrochloric Acid Pretreatment on Different Types of Clay Minerals. *Minerals* **2022**, *12*, 1167. [[CrossRef](#)]
66. Cavender, P.F.; Spears, D.A. Analysis of Forms of Sulphur within Coal, and Minor and Trace Element Associations with Pyrite by ICP Analysis of Extraction Solutions. In *Coal Science and Technology*; Pajares, J.A., Tascón, J.M.D., Eds.; Coal Science; Elsevier: Amsterdam, The Netherlands, 1995; Volume 24, pp. 1653–1656.
67. Grawunder, A.; Merten, D.; Büchel, G. Origin of Middle Rare Earth Element Enrichment in Acid Mine Drainage-Impacted Areas. *Environ. Sci. Pollut. Res.* **2014**, *21*, 6812–6823. [[CrossRef](#)]
68. Yang, J.; Montross, S.; Verba, C. Assessing the Extractability of Rare Earth Elements from Coal Preparation Fines Refuse Using an Organic Acid Lixiviant. *Min. Metall. Explor.* **2021**, *38*, 1701–1709. [[CrossRef](#)]
69. Zhang, W.; Honaker, R. Calcination Pretreatment Effects on Acid Leaching Characteristics of Rare Earth Elements from Middlings and Coarse Refuse Material Associated with a Bituminous Coal Source. *Fuel* **2019**, *249*, 130–145. [[CrossRef](#)]
70. King, J.F.; Taggart, R.K.; Smith, R.C.; Hower, J.C.; Hsu-Kim, H. Aqueous Acid and Alkaline Extraction of Rare Earth Elements from Coal Combustion Ash. *Int. J. Coal Geol.* **2018**, *195*, 75–83. [[CrossRef](#)]
71. Pan, J.; Hassas, B.V.; Rezaee, M.; Zhou, C.; Pisupati, S.V. Recovery of Rare Earth Elements from Coal Fly Ash through Sequential Chemical Roasting, Water Leaching, and Acid Leaching Processes. *J. Clean. Prod.* **2021**, *284*, 124725. [[CrossRef](#)]
72. Taggart, R.K.; Hower, J.C.; Hsu-Kim, H. Effects of Roasting Additives and Leaching Parameters on the Extraction of Rare Earth Elements from Coal Fly Ash. *Int. J. Coal Geol.* **2018**, *196*, 106–114. [[CrossRef](#)]
73. Tang, M.; Zhou, C.; Pan, J.; Zhang, N.; Liu, C.; Cao, S.; Hu, T.; Ji, W. Study on Extraction of Rare Earth Elements from Coal Fly Ash through Alkali Fusion–Acid Leaching. *Miner. Eng.* **2019**, *136*, 36–42. [[CrossRef](#)]

Disclaimer/Publisher’s Note: The statements, opinions and data contained in all publications are solely those of the individual author(s) and contributor(s) and not of MDPI and/or the editor(s). MDPI and/or the editor(s) disclaim responsibility for any injury to people or property resulting from any ideas, methods, instructions or products referred to in the content.